26th International Conference
ENGINEERING MECHANICS 2020
Brno, Czech Republic, November 24 – 25, 2020

VERIFICATION OF THE GEOMETRY OF SAMPLES FOR THE STUDY OF TRABECULAR BONE STRUCTURES

Cichański A.*, Nowicki K.**

Abstract: *Indicators of trabecular bone structure along with the apparent Young's modulus may be a predictor of the risk of bone fracture in the elderly. The use of mechanical treatment in the process of obtaining a sample of a structure to determine these indicators causes damage to its surface, leading to defects in the shape and position of the outline. The paper presents the results of studies leading to the demonstration of the influence of these defects on the values of the BV/TV and the apparent Young's modulus. These results justify the necessity to select the theoretical shape of a cylinder from the scanned images in order to define the geometrical shape of a representative sample. The paper presents a method for determining the parameters of this cylinder based on the best-fit cylinder algorithm.*

Keywords: Bone structure reconstruction, Sample geometry, Best-fit cylinder.

1. Introduction

The clinical standard for determining fracture risk is the bone mineral density aBMD as assessed by DXA dual energy x-ray absorptiometry. The limited effectiveness of this approach is due to the fact that bone fragility is caused not only by low content of the mineral fraction but also by deterioration of bone structure. The microarchitecture of cortical and trabecular bones is a good predictor of fracture risk in the elderly (Samelson et al., 2019). The trabecular structure indices determined as a result of the research are characterized by a higher correlation with strength than the content of the mineral fraction alone. (Topoliński et al., 2012). Grouping structure indicators with the PCA algorithm allows to increase their predictive efficiency based on correlation (Cichanski et al., 2010).

The heterogeneous distribution of the mineral fraction causes regional changes in the properties of the trabecular bone which affect the compressive strength. For vertebral bone values of BV/TV, and E in centrum were significantly smaller for the anterior region than for the posterior region (Kim et al., 2007). For this reason, it should be expected that not only the place of sample collection, but also its form and dimensions may affect the determined values of the apparent modulus and the content of the mineral fraction as well as some other structure indicators. Computer-based μFE analyzes of trabecular structures are performed with cylindrical and cubic samples. The cylindrical samples found in the literature most often have a diameter of 8 mm and a length from 10 mm (Kim et al., 2004) to 20 mm (Bevill and Keaveny, 2009). Another approach is to use cube-shaped samples cut from a cylinder. A cube with a side of 5.28 mm obtained from a cylinder with a diameter of 8 mm was used in the work (Chevalier et al., 2009), and a cube with a side of 5.6 mm obtained from a cylinder with a diameter of 8.5 mm was used in the work (Depalle et al., 2013).

The paper deals with the issue of verification of the diameter of a cylindrical sample due to the correct mapping of the mechanical properties of the trabecular bone structure during numerical analyzes. The apparent Young's modulus and the BV/TV indicator were tested in a wide range of variability of the radius of the sample of the trabecular structure. At the stage of processing the μCT images, the best-fit cylinder algorithm was proposed to determine the geometry of the sample of the trabecular bone structure without any defects in shape and position.

* Assist. Prof. Artur Cichański, PhD.: University of Science and Technology, Faculty of Mechanical Engineering, Kaliskiego 7; 85-796, Bydgoszcz; PL, e-mail: artur.cichanski@utp.edu.pl

** Assist. Prof. Krzysztof Nowicki, PhD.: University of Science and Technology, Faculty of Mechanical Engineering, Kaliskiego 7; 85-796, Bydgoszcz; PL, e-mail: krzysztof.nowicki@utp.edu.pl

2. Materials

Samples of the trabecular structure taken from the neck of the human femur were examined. A set of 46 samples of structures burdened with two diseases was obtained: 15 osteoporosis and 31 coxarthrosis. The samples were cylinders with a diameter of 10 mm and a height of 8.5 mm. The sample preparation procedure is described in the paper (Topoliński et al., 2012). After the cutting out, the samples of the trabecular structure were examined with a resolution of 36 μm on the μCT80 microtomograph. For each of the structure samples, a set of 230 images was obtained, which were then converted to binary form by thresholding, assuming the threshold value as 18% of the maximum brightness.

The research was carried out on the basis of 5 samples selected from set n = 46 on the basis of the BV/TV indicator. Selected samples and their trabecular structure indices are presented in the Tab. 1.

Tab. 1: Selected structure indicators for the analyzed samples.

Sample	Disease	BV/TV, -	Tb.Th, mm	TB.N, 1/mm	Conn.D, -
P_{10} of BV/TV	osteop.	0.1312	0.1433	0.9485	0.9160
P_{30} of BV/TV	coxart.	0.1686	1.0183	0.8164	2.1510
P_{60} of BV/TV	osteop.	0.2065	0.1815	1.1379	1.9552
P_{80} of BV/TV	coxart.	0.2518	1.3653	0.5480	4.0375
P_{100} of BV/TV	coxart.	0.3532	1.4967	0.4321	3.9798

3. Methods

3.1. Test conditions

The research consisted in determining the BV/TV structure indicator and the apparent Yong modulus for cylindrical samples. The cylinders were 7.74 mm long. In the course of the research, its diameter changed in the range from 9.72 mm to 6.7 mm in steps of 0.216 mm. At work (Cichański and Nowicki, 2019) it was shown that at the stage of preparing the μFE model, some μCT scans can be omitted without losing significant information about the mechanical properties of the modeled structure. However, the range of such skip should not be greater than 0.216 mm.

The BV/TV structure index was determined from the thresholded images by the direct method. The apparent Young's modulus was determined numerically by the finite element method in the ANSYS program environment. The mesh for the analyzes was created by directly converting voxel geometry to an element. Eight-node hexahedral elements with a size of 36 μm and isotropic material properties E = 10GPa and ν = 0.3 were used for the analysis. During the analyzes, the cylindrical samples were compressed in the axial direction ε = 0.8 % (Topoliński et al., 2012).

3.2. Best-fit cylinder

A three-dimensional matrix is used to determine the cylinder of best fit, which is a digital image of the sample structure. It was assumed that a matrix cell with a written value greater than 0 symbolizes the mineral part of the bone. In the first step, layers are removed from the matrix, oriented along successive axes of the three-dimensional matrix, which do not contain cells with values greater than 0. Thus, are obtained from the matrix, representing the cuboid described on the sample structure. It was also assumed that half of the length of the shorter side of the base of the cuboid is the maximum radius of the cylinder describing the sample structure - denoted as r_{max}. Then, individual layers of the three-dimensional matrix, selected along the height of the sample, were analyzed. Treating each layer as an image, a Sobel filter was applied to define the edges of the sample edge on that layer. Using the x_{in} and y_{in} coordinates of the sample edge points, the mean square error minimization algorithm was used, determining the location of the centre a_n, b_n and the radius r_n of the circle of the best fit. The error function defining the sum of radial errors for individual points of the sample edge in the form (1) was minimized:

$$\rho_n = \min \sum_i ((x_{in} - a_n)^2 + (y_{in} - b_n)^2) - r_n^2 \quad (1)$$

where:

i – index of the point forming the edge of the sample,

n – index of the analyzed layer.

As a result of the calculations, vectors a_n, b_n and r_n are created with a length n equal to the number of layers, which successively determine the location of the center and the radius of the circle of the best fit on the individual layers of the matrix. It was assumed that the positions of the center of the cylinder of the best fit are determined by the maximum values in the vectors a_n and b_n, respectively, while the radius of the cylinder of the best fit is determined by the minimum value in the vector r_n.

4. Results

As a result of processing the binary images, it was determined how the BV/TV values changed with the decrease of the sample diameter. The results obtained are shown in Fig. 1a) by the relative values related to BV/TV determined for the largest diameter D_{max} = 9.72 mm. Fig. 1b) shows in a similar convention the changes in the value of the apparent Young's modulus E_{app} determined during the μFE analyzes.

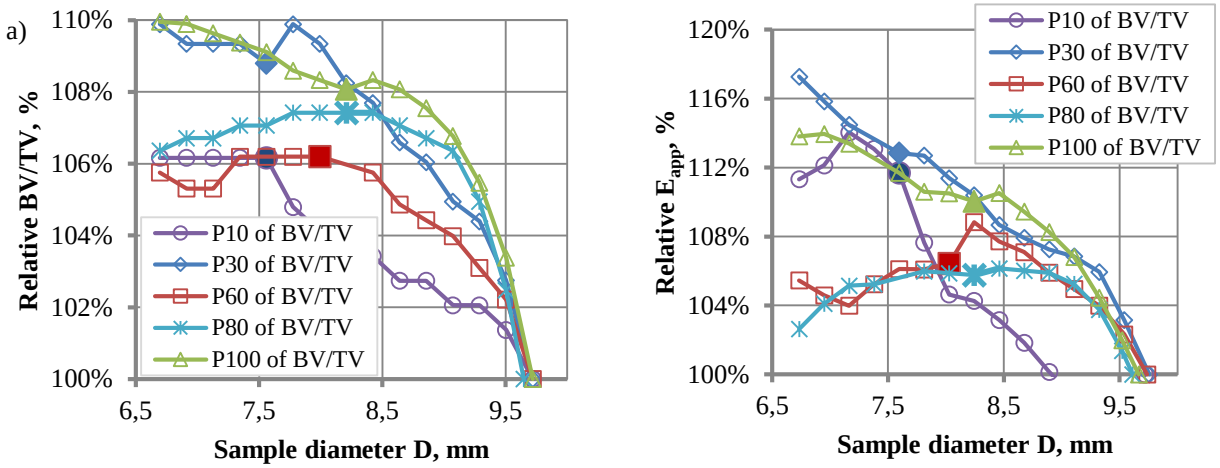

Fig. 1: Relative values of: a) BV/TV indicator, b) E_{app} apparent Young's modulus.

As a result of applying the best-fit cylinder algorithm, appropriate values of the D_n diameters were determined. The obtained results are presented for selected samples in Tab. 2. On the courses of relative values shown for individual samples in Fig. 1, points corresponding to the best-fit cylinder diameters were distinguished by means of filled markers.

Tab. 2: Best-fit cylinder diameters.

	Sample				
	P_{10} of BV/TV	**P_{30} of BV/TV**	**P_{60} of BV/TV**	**P_{80} of BV/TV**	**P_{100} of BV/TV**
Diameter D_n	7.56 mm	7.632 mm	7.992 mm	8.28 mm	8.208 mm

Analysis of the position of the points corresponding to the best-fit cylinder diameters D_n in the BV/TV relative plots (Fig 1a) shows that these points divide the corresponding curves into two ranges. In the range from D_{max} to D_n, the values of BV/TV increases dynamically. In the range of diameters below D_n, the BV/TV values slightly increase for samples P_{30} and P_{100}, they stabilize for samples P_{10} and P_{60} and even decrease as it is for samples P_{80}. The BV/TV values calculated using the samples with the D_{max} are on average low by 7 % compared to the BV/TV values calculated using the samples with the D_n. A similar division into the two ranges of the relative E_{app} plots due to the distinction of points corresponding to the best-fit cylinder diameters D_n can be seen in Fig 1b). The apparent Young's modulus E_{app} values for samples with D_{max} diameter are on average 9% lower than the E_{app} values for samples with D_n diameter.

5. Conclusions

Due to the use of mechanical treatment of biological material in the process of obtaining a sample to determine indicators of the trabecular structure, damage appears on its surface. This damage leads to shape defects of the sample outline. The method of cutting out samples also does not ensure the parallelism of the bases of the cylinder and the perpendicularity of the bases and the generatrix of the cylinder. Therefore, it is necessary to select the theoretical shape of the cylinder from the scanned images. The paper presents a method for determining the parameters of this cylinder based on the best-fit cylinder algorithm.

Determination of the trabecular bone structure indices with the use of samples with a diameter resulting from the cutting process leads to an underestimation of the BV/TV index for the structure under study. On the surfaces of such samples, there are areas in which the mineral fraction BV is missing, which, at a given volume of TV, leads to an underestimation of the BV/TV ratio. Further research should be carried out on how the indicated effect influences the values of other indices of the trabecular structure.

Deficiencies of the mineral fraction in some sections of the sample contribute to the reduction of its stiffness. This leads to the underestimation of the apparent Young's modulus determined in the μFE analysis. The use of the best-fit cylinder algorithm makes it possible to indicate the diameter of the sample so that its entire volume is filled with the mineral fraction in a manner resulting from the bone structure contained in the sample outline.

References

Bevill, G. and Keaveny, T. (2009) Trabecular bone strength predictions using finite element analysis of micro-scale images at limited spatial resolution, Bone, 44, 4, pp. 579-584.

Chevalier, Y., Pahr D. and Zysset, P. (2009) The role of cortical shell and trabecular fabric in finite element analysis of the human vertebral body, Journal of Biomechanical Engineering, 131, 11, 111003.

Cichański, A. and Nowicki, K. (2019) Trabecular bone microstructural FEM analysis for out-of plane resolution change, In: Arkusz K, Bedzinski R, Klekiel T, Piszczatowski S (eds), Biomechanics in Medicine and Biology, Springer, Advances in Intelligent Systems and Computing, 831, pp. 210-218.

Cichański, A., Nowicki, K., Mazurkiewicz, A. and Topolinski, T. (2010) Investigation of statistical relationships between quantities describing bone architecture, its fractal dimensions and mechanical properties, Acta of Bioengineering and Biomechanics, 12, 4, pp. 69-77.

Depalle, B., Chapurlat, R., Walter-Le-Berre, H., Bou-Said, B. and Follet, H. (2013) Finite element dependence of stress evaluation for human trabecular bone, Journal of the Mechanical Behavior of Biomedical Materials, 18, pp. 200-212.

Kim, D., Christopherson, G., Dong, X., Fyhrie, D. and Yeni, Y. (2004) The effect of microcomputed tomography scanning and reconstruction voxel size on the accuracy of stereological measurements in human cancellous bone, Bone, 35, 6, pp. 1375-1382.

Kim, D., Hunt, C., Zauel, R., Fyhrie, D. and Yeni, Y. (2007) The effect of regional variations of the trabecular bone properties on the compressive strength of human vertebral bodies, Annals of Biomedical Engineering, 35, 11, pp. 1907-1913.

Samelson, E., Broe, K., Xu, H., Yang, L., Boyd, S., Biver, E., Szulc, P., Adachi, J., Amin, S., Atkinson, E., Berger, C., Burt, L., Chapurlat, R., Chevalley, T., Ferrari, S., Goltzman, D., Hanley, D., Hannan, M., Khosla, S., Liu, C., Lorentzon, M., Mellstrom, D., Merle, B., Nethander, M., Rizzoli, R., Sornay-Rendu, E., Van Rietbergen, B., Sundh, D., Wong, A., Ohlsson, C., Demissie, S., Kiel, D. and Bouxsein, M. (2019) Cortical and trabecular bone microarchitecture as an independent predictor of incident fracture risk in older women and men in the Bone Microarchitecture International Consortium (BoMIC): a prospective study, Lancet Diabetes Endocrinol, 7, 1, pp. 34-43.

Topoliński, T., Cichański, A., Mazurkiewicz, A. and Nowicki, K. (2012) The relationship between trabecular bone structure modeling methods and the elastic modulus as calculated by FEM, The Scientific World Journal, 827196.

Topoliński, T., Mazurkiewicz, A., Jung, S., Cichański, A. and Nowicki, K. (2012) Microarchitecture Parameters Describe Bone Structure and Its Strength Better Than BMD, The Scientific World Journal, 502781.